Falkland Islands Fisheries Department

Loligo **Stock Assessment, Second Season 2014**

Andreas Winter

October 2014

Index

Summary

1) The second season *Loligo* fishery of 2014 was open for the scheduled 71 days from July 22nd to September 30th. This season marked the second half of a scheduling change as the fishery was shortened by one week off the start, offsetting the first season which was extended one week longer to the end.
2) 19,630 tonnes of *Loligo* catch were reported in the X-license fishery; marginally higher than the year before and the median second-season catch total of the last five years. Throughout the season 44.3% of *Loligo* catch and 47.6% of fishing effort were taken north of latitude 52° S; 55.7% of *Loligo* catch and 52.4% of fishing effort were taken south of 52° S.
3) Sub-areas north and south of 52° S were depletion-modelled separately. In the north sub-area, three depletion periods were inferred to have started on July 24th, August 16th, and September 18th. In the south sub-area, three depletion periods were inferred to have started on July 28th, August 14th, and September 15th.
4) Approximately 9,414 tonnes of *Loligo* (95% confidence interval: [0 to 23,837] tonnes) were estimated to have immigrated into the Loligo Box during first season 2014, representing 19% of the *Loligo* biomass in the fishing zone.
5) The final total estimate for *Loligo* remaining in the Loligo Box at the end of second season 2013 was:
Maximum likelihood of 17,250 tonnes, with a 95% confidence interval of [13,250 to 28,500] tonnes.
The risk of *Loligo* escapement biomass at the end of the season being less than 10,000 tonnes was estimated at effectively zero.

Introduction

The second season of the 2014 *Loligo* fishery (*Doryteuthis gahi* – Patagonian squid) opened on July 22nd with all 16 X-licensed vessels participating; none taking the flex option to start later. Season opening was one week later than second season of previous years, complementary to the scheduling change of one week having been added to the end of first season (Winter, 2014). The season ended by directed closure on September 30th. During the season, one vessel was substituted for repairs by a slightly larger vessel, for a period of 10 days. One vessel, with observer onboard, took three exploratory fishing days north of the Loligo Box with permission from the FIFD. Total reported *Loligo* catch by X-licensed vessels in the 2014 second season was 19,630 tonnes in 1099 vessel-days (Table 1); giving an intermediate catch rate by comparison of the last five second seasons.

As in previous seasons, the *Loligo* stock assessment was conducted with depletion time-series models (Agnew et al., 1998; Roa-Ureta and Arkhipkin, 2007; Arkhipkin et al., 2008). Because *Loligo* has an annual life cycle (Patterson, 1988), stock cannot be derived from a standing biomass carried over from prior years (Rosenberg et al., 1990). The depletion model instead calculates an estimate of population abundance over time by evaluating what levels of abundance and catchability must be extant to sustain the observed rate of catch. Depletion modelling is used both in-season and for the post-season summary, with the objective of maintaining an escapement biomass of 10,000 tonnes *Loligo* at the end of each season as a conservation threshold (Agnew et al., 2002; Barton, 2002).

Table 1. *Loligo* season comparisons since 2004. Days: total number of calendar days open to licensed *Loligo* fishing including (since 1st season 2013) optional extension days; V-Days: aggregate number of licensed *Loligo* fishing days reported by all vessels for the season.

| | Season 1 | | | Season 2 | | |
	Catch (t)	Days	V-Days	Catch (t)	Days	V-Days
2004				17,559	78	1271
2005	24,605	45	576	29,659	78	1210
2006	19,056	50	704	23,238	53	883
2007	17,229	50	680	24,171	63	1063
2008	24,752	51	780	26,996	78	1189
2009	12,764	50	773	17,836	59	923
2010	28,754	50	765	36,993	78	1169
2011	15,271	50	771	18,725	70	1099
2012	34,767	51	770	35,026	78	1095
2013	19,908	53	782	19,614	78	1195
2014	28,119	59	872	19,630	71	1099

Methods

The depletion model formulated for the Falkland Islands *Loligo* stock is based on the equivalence:

$$C_{day} = q \times E_{day} \times N_{day} \times e^{-M/2} \tag{1}$$

where q is the catchability coefficient, M is the natural mortality rate (considered constant at 0.0133 day^{-1}; Roa-Ureta and Arkhipkin, 2007), and C_{day}, E_{day}, N_{day} are catch (numbers of *Loligo*), fishing effort (numbers of vessels), and abundance (numbers of *Loligo*) per day. In its basic form (DeLury, 1947) the depletion model assumes a closed population in a fixed area for the duration of the assessment. However, the assumption of a closed population is imperfectly met in the Falkland Islands fishery, where stock analyses have often shown that *Loligo* groups arrive in successive waves after the start of the season (Roa-Ureta, 2012; Winter and Arkhipkin, 2012). Arrivals of successive groups are inferred from discontinuities in the catch data. Fishing on a single, closed cohort would be expected to yield gradually decreasing CPUE, but gradually increasing average individual sizes, as the squid grow. When instead these data change suddenly, or in contrast to expectation, the immigration of a new group to the population is indicated.

In the event of a new group arrival, the depletion calculation must be modified to account for this influx. This was done using a simultaneous algorithm (Roa-Ureta, 2012) that adds new arrivals on top of the stock previously present, and posits a common catchability coefficient for the entire depletion time-series. If two depletions are included in the same model (i.e., the stock present from the start plus a new group arrival), then:

$$C_{day} = q \times E_{day} \times (N1_{day} + (N2_{day} \times i2|_0^1)) \times e^{-M/2} \tag{2}$$

where i2 is a dummy variable taking the values 0 or 1 if 'day' is before or after the start day of the second depletion. For more than two depletions, $N3_{day}$, i3, $N4_{day}$, i4, etc., would be included following the same pattern.

The *Loligo* stock assessment was calculated in a Bayesian framework (Punt and Hilborn, 1997), whereby results of the season depletion model are conditioned by prior information on the stock; in this case the information from the pre-season survey. The season depletion likelihood function was calculated as the difference between actual catch numbers reported and catch numbers predicted from the model (equation **2**), statistically corrected by a factor relating to the number of days of the depletion period (Roa-Ureta, 2012):

$$((n\text{Days} - 2)/2) \times \log\left(\sum_{days}\left(\log(\text{predicted } C_{day}) - \log(\text{actual } C_{day})\right)^2\right) \qquad \textbf{(3)}$$

The survey prior likelihood function was calculated as the normal distribution of the difference between catchability (q) derived from the survey abundance estimate, and catchability derived from the season depletion model:

$$\frac{1}{\sqrt{2\pi \cdot SD_{q\,survey}{}^2}} \times \exp\left(-\frac{\left(q_{model} - q_{survey}\right)^2}{2 \cdot SD_{q\,survey}{}^2}\right) \qquad \textbf{(4)}$$

Catchability, rather than abundance N, was used for calculating the survey prior likelihood because catchability informs the entire season time series; whereas N from the survey only informs the first season depletion period – subsequent immigrations and depletions are independent of the abundance that was present during the survey.

Bayesian optimization of the depletion was calculated by jointly minimizing equations **3** and **4**, using the Nelder-Mead algorithm in R programming package 'optimx' (Nash and Varadhan, 2011). Relative weights in the joint optimization were assigned to equations **3** and **4** as the converse of their coefficients of variation (CV), i.e., the CV of the prior became the weight of the depletion model and the CV of the depletion model became the weight of the prior. Calculations of the CVs are described in the Appendix.

With C_{day}, E_{day} and M being fixed parameters, the optimization of equation **2** using equations **3** and **4** produces estimates of q and N1, N2, …, etc. Numbers of *Loligo* on the final day (or any other day) of a time series are then calculated as the numbers N of the depletion start days discounted for natural mortality during the intervening period, and subtracting cumulative catch also discounted for natural mortality (CNMD). Taking for example a two-depletion period:

$$N_{final\,day} = N1_{start\,day\,1} \times e^{-M(final\,day\,-\,start\,day\,1)}$$
$$+ \; N2_{start\,day\,2} \times e^{-M(final\,day\,-\,start\,day\,2)}$$
$$- \; CNMD_{final\,day} \qquad \textbf{(5)}$$

where

$$CNMD_{day\,1} = 0$$
$$CNMD_{day\,x} = CNMD_{day\,x-1} \times e^{-M} + C_{day\,x-1} \times e^{-M/2} \qquad \textbf{(6)}$$

N $_{final\ day}$ is then multiplied by the average individual weight of *Loligo* on the final day to give biomass. Daily average individual weight is obtained from length / weight conversion of mantle lengths measured in-season by observers, and also derived from in-season commercial data as the proportion of product weight that vessels reported per market size category. Observer mantle lengths are scientifically precise, but restricted to 1-2 vessels at any one time that may or may not be representative of the entire fleet. Commercially proportioned mantle lengths are relatively less precise, but cover the entire fishing fleet. Therefore, both sources of data are used. Daily average individual weights are calculated by averaging observer size samples and commercial size categories where observer data are available, otherwise only commercial size categories. A modification to the algorithm was applied this season by multiplying the expected value of the average individual weight from its GAM trend (see Appendix) rather than the empirical value on each day, to smooth fluctuations.

Distributions of the likelihood estimates from joint optimization (i.e., measures of their statistical uncertainty) were computed using a Markov Chain Monte Carlo (MCMC) (Gamerman and Lopes, 2006), a method that is commonly employed for fisheries assessments (Magnusson et al., 2013). MCMC is an iterative process which generates random stepwise changes to the proposed outcome of a model (in this case, the N and q of *Loligo*) and at each step, accepts or nullifies the change with a probability equivalent to how well the change fits the model parameters compared to the previous step. The resulting sequence of accepted or nullified changes (i.e., the 'chain') approximates the likelihood distribution of the model outcome. The MCMC of the depletion models were run for 100,000 iterations; the first 1000 iterations were discarded as burn-in sections (initial phases over which the algorithm stabilizes); and the chains were thinned by a factor equivalent to the maximum of either 5 or the inverse of the acceptance rate (e.g., if the acceptance rate was 12.5%, then every 8th (0.125^{-1}) iteration was retained) to reduce serial correlation. For each model three chains were run; one chain initiated with the parameter values obtained from the joint optimization of equations **3** and **4**, one chain initiated with these parameters ×2, and one chain initiated with these parameters ×¼. Convergence of the three chains was accepted if the variance among chains was less than 10% higher than the variance within chains (Brooks and Gelman, 1998). When convergence was satisfied the three chains were combined as one final set. Equations **5**, **6**, and the multiplication by average individual weight were applied to CNMD and each iteration of N values in the final set, and the biomass outcomes from these calculations represent the distribution of the estimate. Maximum likelihood of biomass on each day was defined as the peak of the histogram of MCMC outcomes at 500-tonne intervals.

Total escapement biomass is defined as the aggregate biomass of *Loligo* on the last day of the season for north and south sub-areas combined. In previous seasons, north and south biomasses were assumed to be independent and therefore the total was calculated by adding the respective north and south likelihood distributions in random order. However, the time series of catch and effort in this season suggested that north and south biomasses are in fact correlated and therefore the likelihood distributions were added semi-randomly in proportion to the strength of the correlation. The semi-randomization is described in the Appendix.

Figure 1 [next page]. Spatial distribution of *Loligo* 2ⁿᵈ-season commercial catches, colour-scaled to catch weight (maximum = 31.9 tonnes). 3913 trawl catches were taken during the season. The 'Loligo Box' fishing zone, as well as the 52 ºS parallel delineating the boundary between north and south assessment sub-areas, are shown in gray.

Commercial catch, 22/07 - 30/09 2014
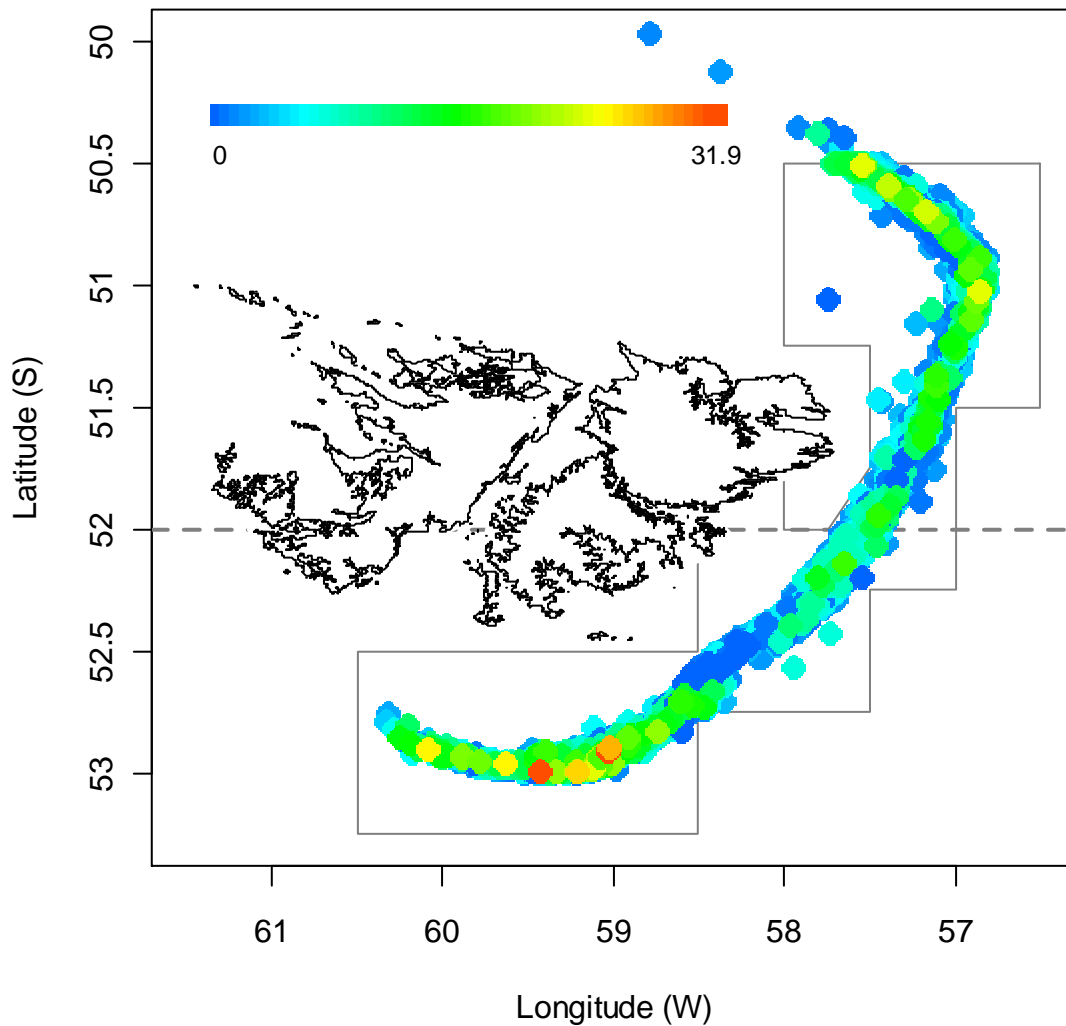
Stock assessment
Data

Fishing effort in the 2nd season of 2014 was distributed more evenly (less segregated north-south) than most recent 2nd seasons (Figure 1), with 13.1% of vessel-days in what was previously (Arkhipkin and Middleton, 2002; Roa-Ureta and Arkhipkin, 2007) designated as the central sub-area of the Loligo Box; south of 52º S and east of 58.5º W. This represents the third-highest percentage of effort in the centre of the past ten 2nd seasons, behind 2006 and 2011, both of which were closed early.

A total of 1099 vessel-days were fished during the season, with a median of 16 vessels per day (Figure 2). On one day of particularly bad weather (August 13th; Figure 3) only 8 vessels fished. Vessels reported daily catch totals to the FIFD and electronic logbook data that included trawl times, positions, and product weight by market size categories. Three FIFD observers were deployed on four vessels in the fishery for a total of 83 observer-days. Throughout the 71 days of the season, 1 day had no observer covering, 57 days had 1 observer covering, and 13 days had two observers covering. Observers sampled an average of 386.7 *Loligo* daily, and reported their maturity stages, sex, and lengths to 0.5 cm. The length-weight relationship for

converting both observer and commercially proportioned length data was taken from the pre-season survey (Winter et al, 2014):

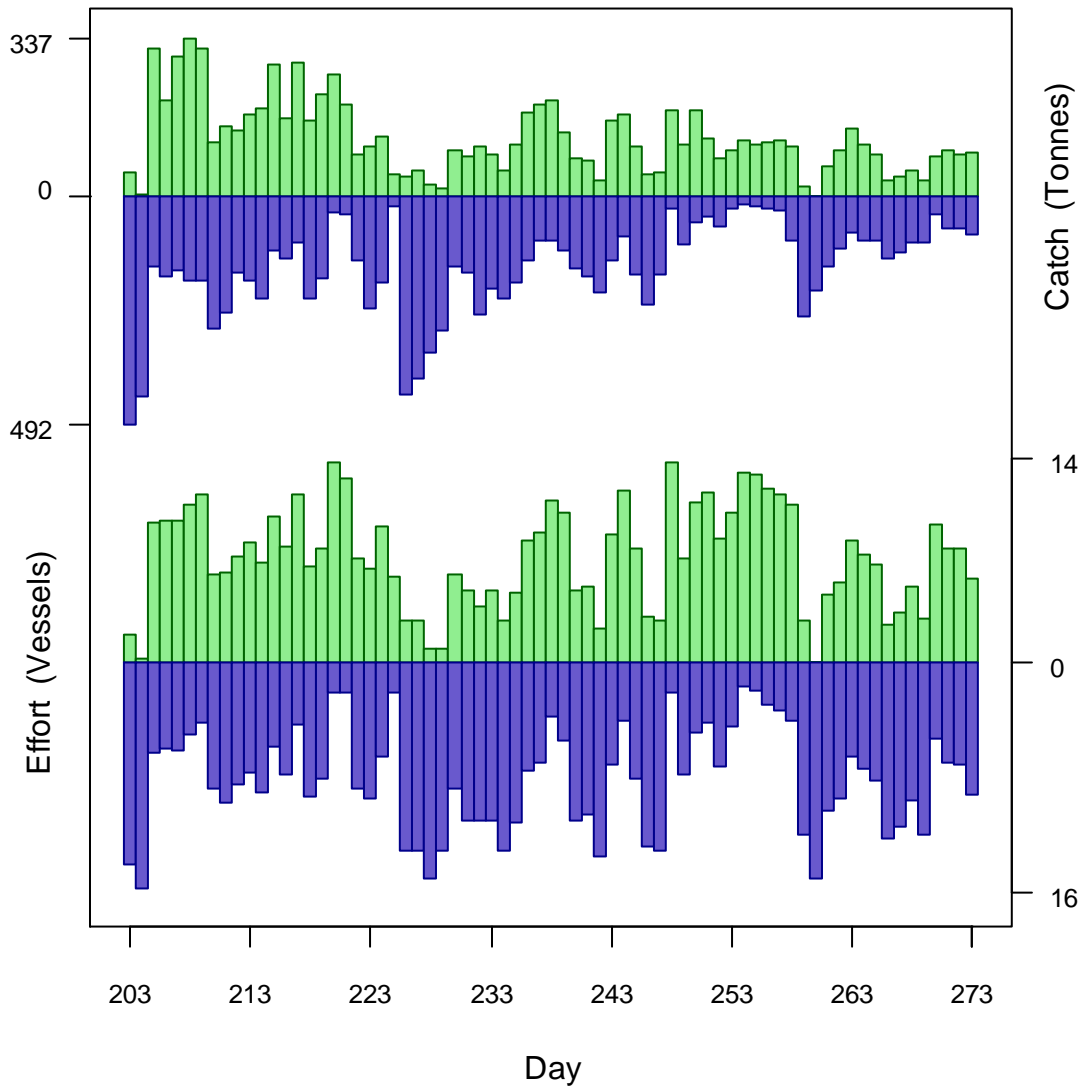$$\text{weight (kg)} = 0.135 \times length \ (cm)^{2.278} / 1000 \tag{7}$$

Figure 2. Daily total *Loligo* catch and effort distribution by assessment sub-area north (green) and south (purple) of the 52º S parallel in the *Loligo* 2nd season 2014. The season was open from July 22nd (chronological day 203) to September 30th (chronological day 273). As many as 14 vessels fished per day north of 52º S; as many as 16 vessels fished per day south of 52º S. As much as 337 tonnes *Loligo* was caught per day north of 52º S; as much as 492 tonnes *Loligo* was caught per day south of 52º S.

This season was characterized by the presence of high numbers of large male *Loligo*, already noted during the pre-season survey (Winter et al., 2014). As these large males were progressively caught or dispersed throughout the season, a relatively unusual trend was obtained of overall average size decreasing instead of increasing with the growth of the new squid (Figure 4).
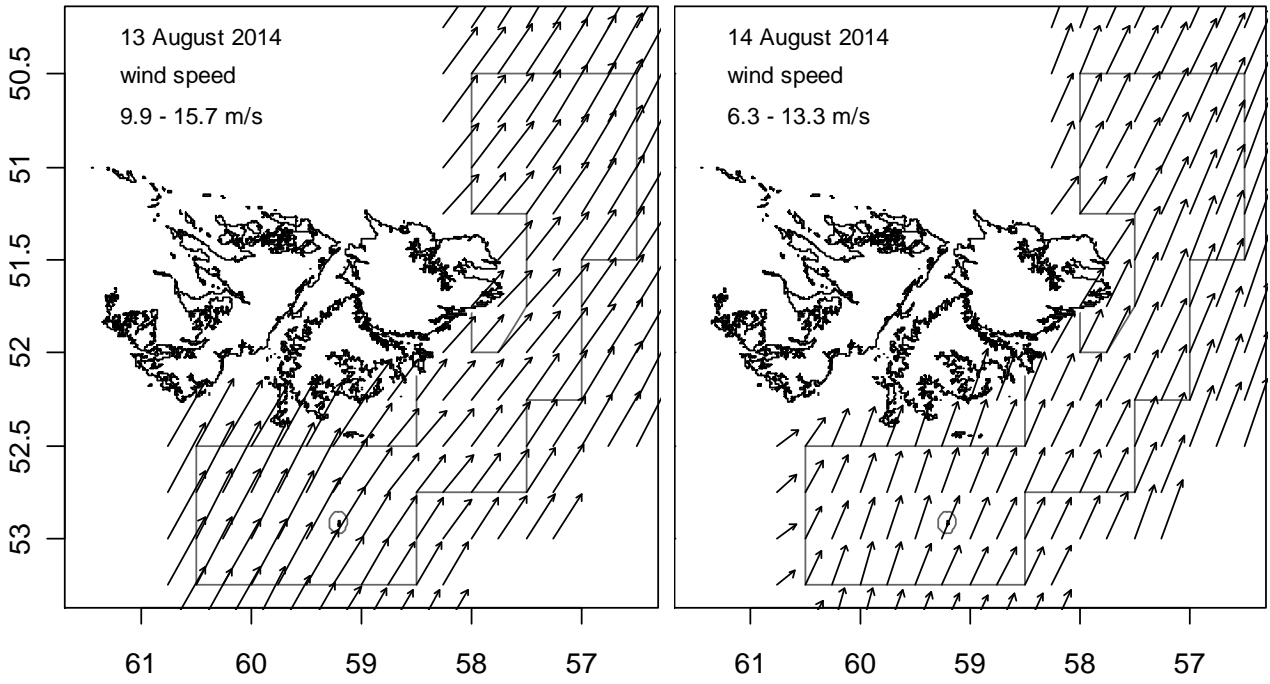
Figure 3. Sea wind vectors at 0.25° resolution, from blended satellite observations (Zhang et al., 2006), on the day that half the fleet stopped fishing to shelter (August 13th), and the day after when fishing resumed by the whole fleet (August 14th).
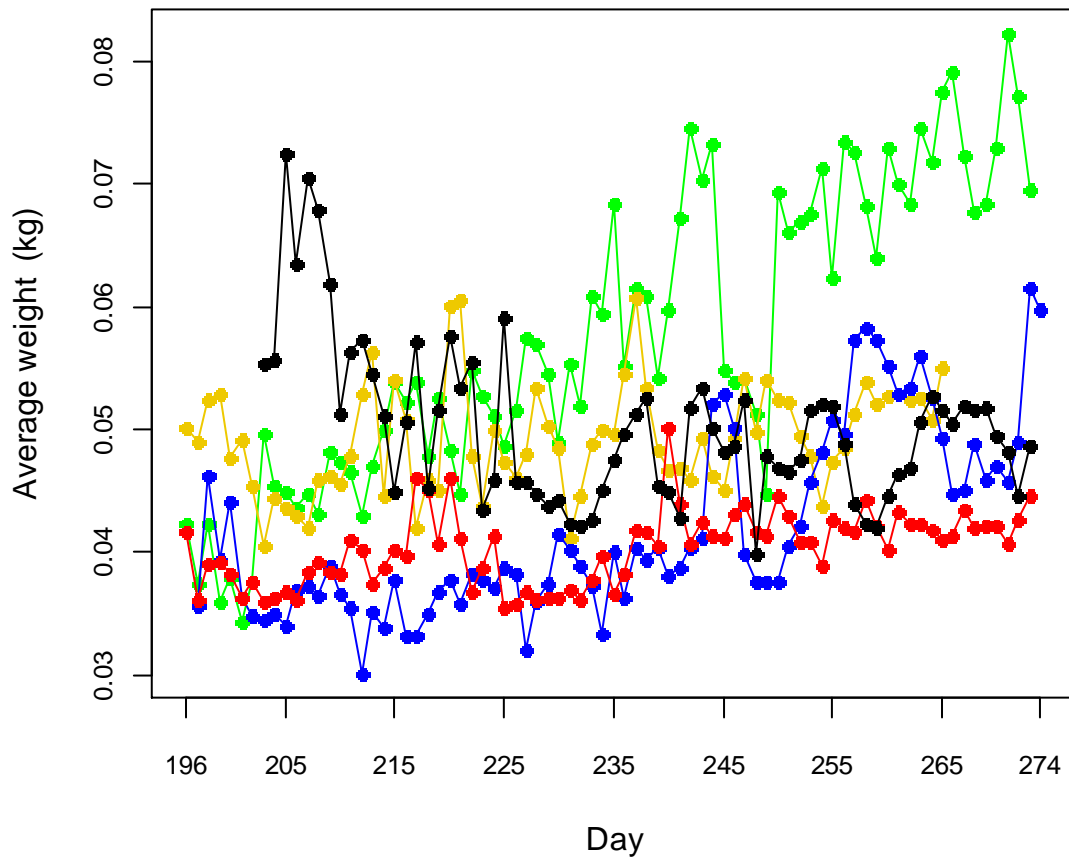
Figure 4 [previous page]. Average individual weights of *Loligo* (male and female, entire fishing zone) in 2nd seasons of 2010 (green), 2011 (gold), 2012 (blue), 2013 (red), 2014 (black). Note that in 2010 average weights were calculated preponderantly from observer measurements, which tend to be higher than commercial size data.


Group arrivals / depletion criteria

Start days of depletions - following arrivals of new *Loligo* groups - were judged primarily with reference to daily changes in CPUE, with additional information from sex proportions, maturity, and average individual *Loligo* sizes. CPUE was calculated as metric tonnes of *Loligo* caught per vessel per day. Days were used rather than trawl hours as the basic unit of effort. Commercial vessels do not trawl standardized duration hours, but rather durations that best suit their daily processing requirements. An effort index of days is therefore more consistent.

Three days in the north and three days in the south were identified that most plausibly represented the onset of separate immigrations / depletions.

- The first in-season depletion north was identified on day 205 (July 24th – two days past the start of the commercial season), after which generally declining trends in average commercial size category weight (Figure 5A) and CPUE (Figure 6) were observed for about three weeks, and observer data showed increasing proportions of size, and maturity of females (Figure 5B, D).
- The second depletion north was identified on day 228 (August 16th) with a CPUE peak, that, although fished by only few vessels, marked a consistent increase over three days (Figure 6). Average commercial weight was one day short of its highest peak in three weeks (Figure 5A).
- The third depletion north was identified on day 261 (September 18th) with the highest CPUE since 10 days earlier (Figure 6) and the start of a 4-day increasing trend in average commercial weight (Figure 5A).
- The first in-season depletion south was identified on day 209 (July 28th) with a CPUE peak that was the highest of the season (Figure 6).
- The second depletion south was identified on day 226 (August 14th) with a strong peak in CPUE (Figure 6), and the day after a local maximum in average commercial weight (Figure 5A).
- The third depletion south was identified on day 258 (September 15th) with another CPUE peak (Figure 6), and near the onset of increasing trends in female proportion and female maturity (Figure 5C, D).

Figure 5 [next page]. A: Average individual *Loligo* weights (kg) per day from commercial size categories. B: Average individual *Loligo* weights (kg) by sex per day from observer sampling. C: Proportions of female *Loligo* per day from observer sampling. D: avg. maturity value by sex per day from observer sampling. In all graphs – Males: triangles, females: squares, unsexed: circles. North sub-area: green, south sub-area: purple. Data from consecutive days are joined by line segments. Broken gray bars indicate days 205, 228 and 261, identified as the start of in-season depletions north. Solid gray bars indicate days 209, 226, and 258, identified as the start of in-season depletions south.
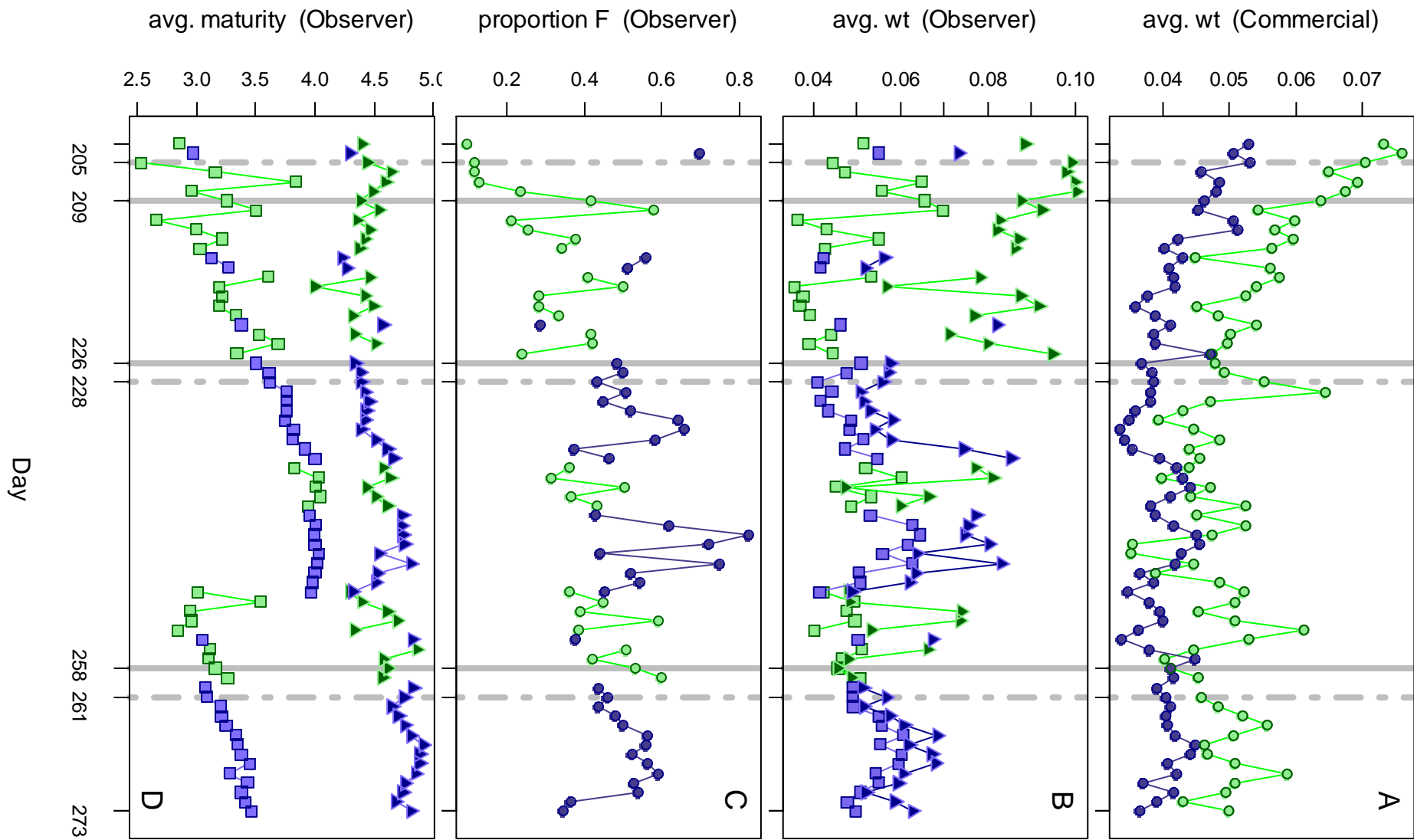
Figure 6. CPUE in metric tonnes per vessel per day, by assessment sub-area north (green) and south (purple) of the 52º S parallel. Circle sizes are proportioned to the numbers of vessel fishing. Data from consecutive days are joined by line segments. Broken gray bars indicate days 205, 228 and 261, identified as the start of in-season depletions north. Solid gray bars indicate days 209, 226, and 258, identified as the start of in-season depletions south.
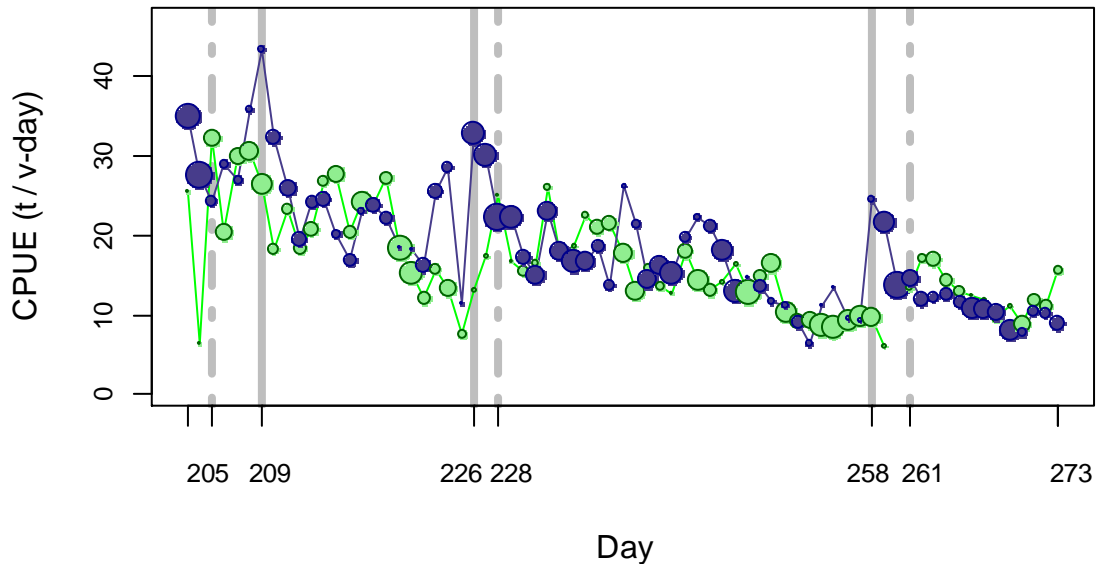
Depletion analyses
North

In the north sub-area, Bayesian optimization on catchability (q) resulted in a posterior (max. likelihood $q_N = 1.275 \times 10^{-3}$; Figure 7, left) that, given the non-linearity of the model, was actually lower than both the pre-season prior ($_{prior} q_N = 1.35 \times 10^{-3}$; Figure 7, left, and equation **A3-N**) and the in-season depletion ($_{depletion} q_N = 1.59 \times 10^{-3}$; Figure 7, left, and **A5-N**). Respective weights in the Bayesian optimization (converse of the CVs) were 0.551 for the in-season depletion (**A4-N**) and 0.253 for the prior (**A8-N**).

The MCMC distribution of the posterior multiplied by the GAM fit of average individual *Loligo* weight on the final day of the season (48.0 g; Figure A2-N), gave the likelihood distribution of *Loligo* final-day biomass shown in Figure 7, right, with maximum likelihood and 95% confidence interval (to the nearest 250 t) of:

$$B_{N\ day\ 273} \qquad = \quad 9{,}250\ t \ \sim\ 95\%\ CI\ [7{,}000 - 15{,}000]\ t \qquad\qquad \textbf{(8)}$$

At its highest point (start of the season; July 22nd), estimated *Loligo* biomass north was 25,250 t ~ 95% CI [20,250 - 41,000] t (Figure 8).

Figure 7 [next page]. North sub-area. Left: Likelihood distributions for *Loligo* catchability. Red line: prior model (pre-season survey data), blue line: in-season depletion model, gray bars: combined Bayesian model. Right: Likelihood distribution (gray bars) of escapement biomass, from Bayesian posterior and average individual *Loligo* weight at the end of the season. Green lines: maximum likelihood and 95% confidence interval. Note the correspondence to Figure 8.
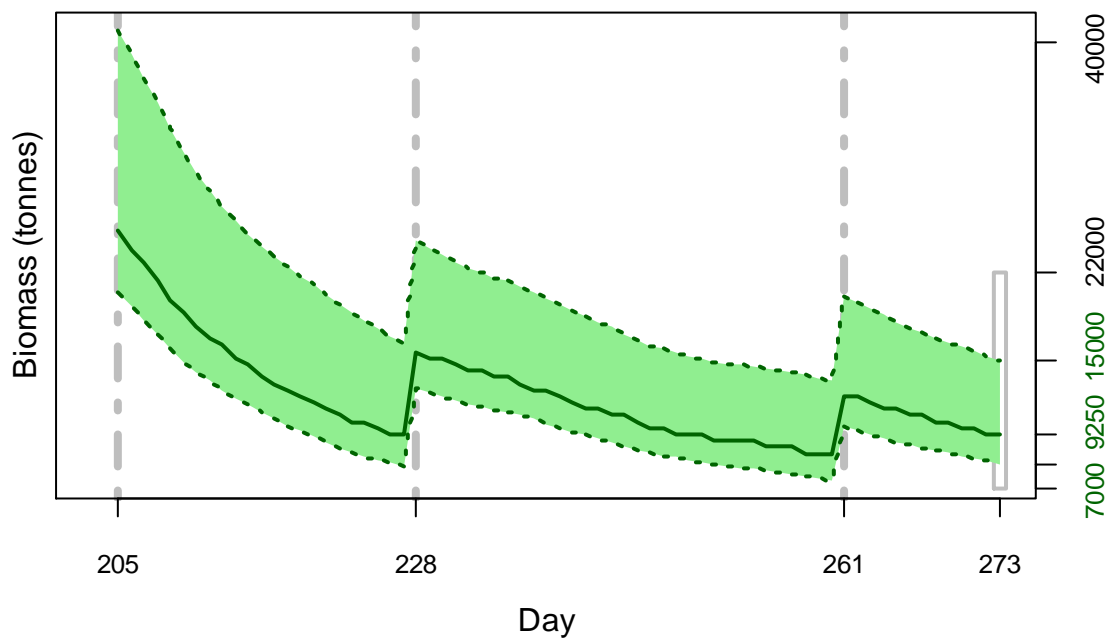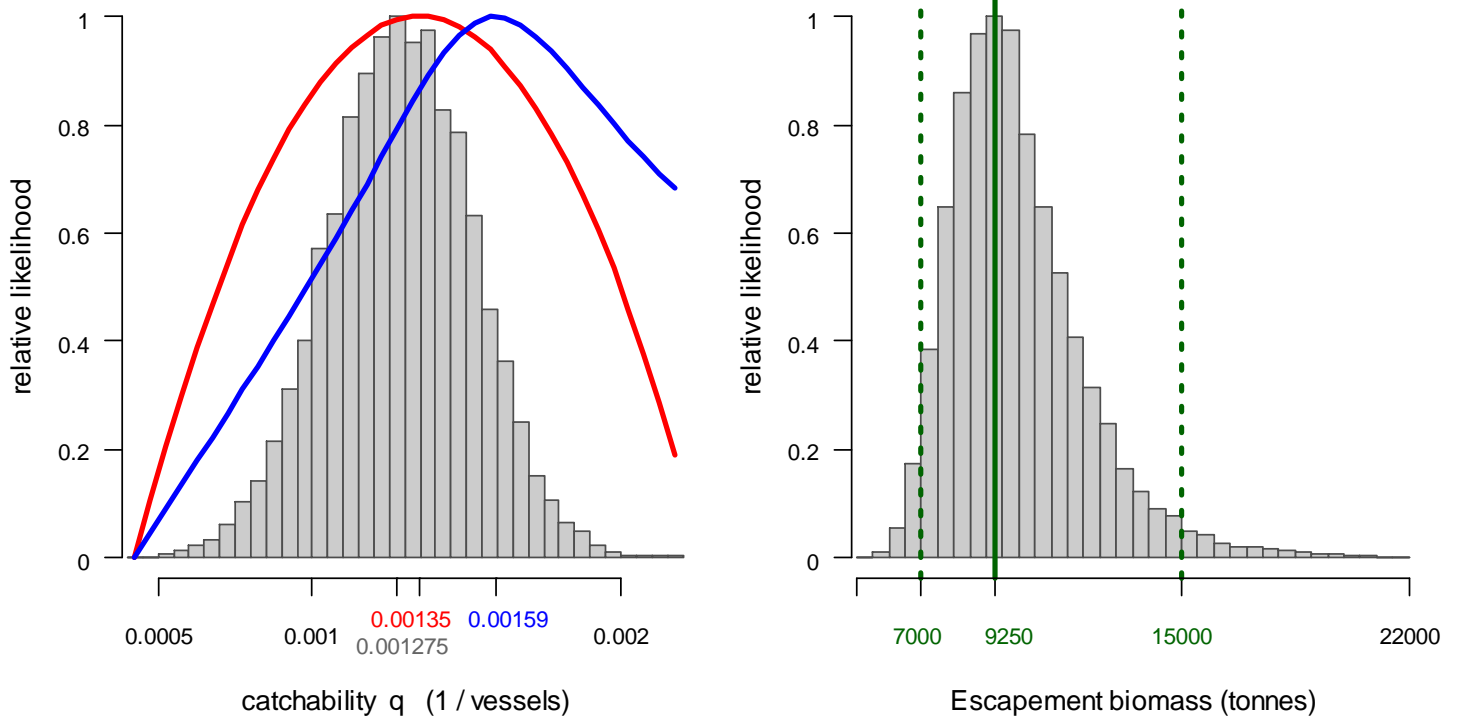
Figure 8. North sub-area. *Loligo* biomass time series estimated from Bayesian posterior of the depletion model ± 95% confidence intervals. Broken gray bars indicate days 205, 228, and 261, identified as the start of in-season depletions north. Note that the biomass 'footprint' on day 273 corresponds to the right-side plot of Figure 7.

South

In the south sub-area, the Bayesian posterior for catchability (q) (max. likelihood $q_S = 1.325 \times 10^{-3}$; Figure 9, left) was also lower than the preseason prior ($_{prior}q_S = 1.392 \times$

10^{-3}; Figure 9, left, and equation **A3-S**) and nearly identical in-season depletion (depletion $q_s = 1.405 \times 10^{-3}$; Figure 9, left, and **A5-S**). Bayesian optimization was weighted 0.600 for in-season depletion (**A4-S**) vs. 0.258 for the prior (**A8-S**).
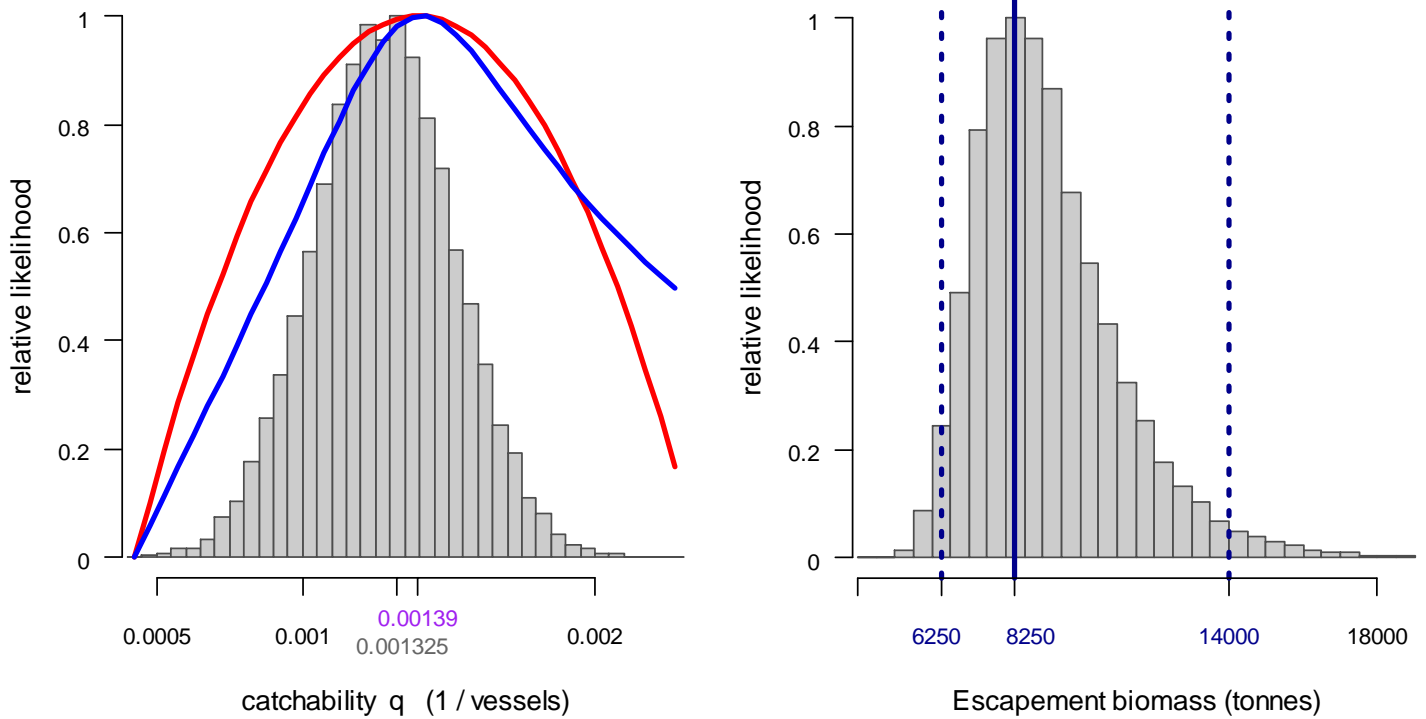

Figure 9. South sub-area. Left: Likelihood distributions for *Loligo* catchability. Red line: prior model (pre-season survey data), blue line: in-season depletion model, gray bars: combined Bayesian model. Right: Likelihood distribution (gray bars) of escapement biomass, from Bayesian posterior and average individual *Loligo* weight at the end of the season. Blue lines: maximum likelihood and 95% confidence interval. Note the correspondence to Figure 10.
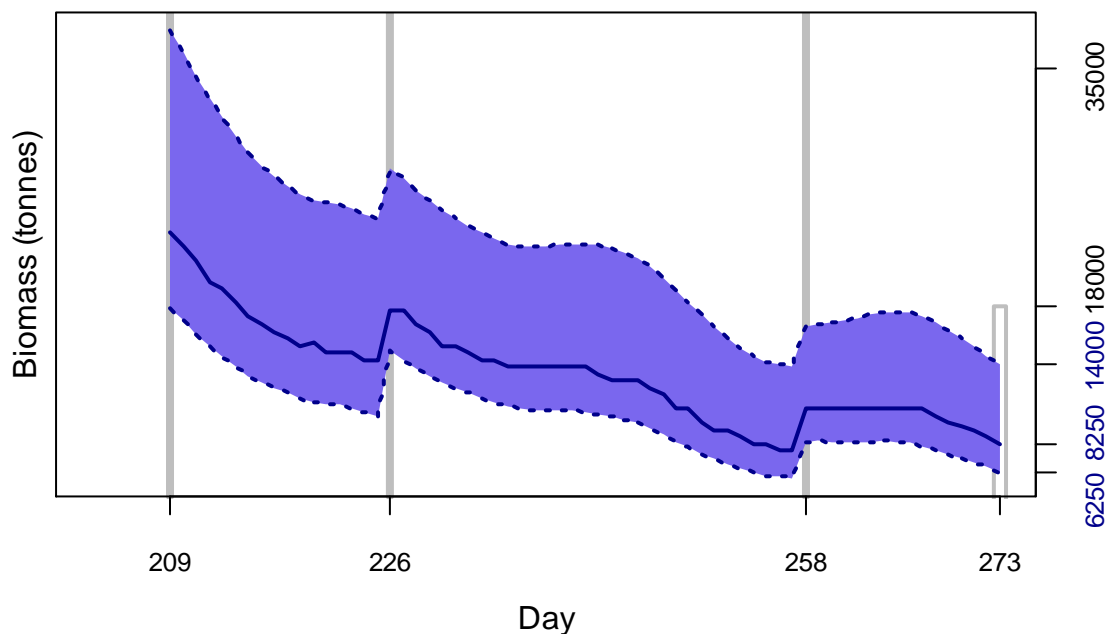
Figure 10 [previous page]. South sub-area. *Loligo* biomass time series estimated from Bayesian posterior of the depletion model ± 95% confidence intervals. Solid gray bars indicate days 209, 226, and 258, identified as the start of in-season depletions south. Note that the biomass 'footprint' on day 273 corresponds to the right-side plot of Figure 9.

The MCMC distribution of the posterior multiplied by average individual *Loligo* weight on the final day of the season (47.0 g; Figure A2-S), gave the likelihood distribution of *Loligo* final-day biomass shown in Figure 9, right, with maximum likelihood and 95% confidence interval of:

$$B_{S\ day\ 273} \quad = \quad 8{,}250\ t \sim 95\%\ CI\ [6{,}250 - 14{,}000]\ t \tag{9}$$

At its highest point (start of the season; July 22nd), estimated *Loligo* biomass south was 23,250 t ~ 95% CI [17,750 - 37,750] t (Figure 10).

Escapement biomass

Total escapement biomass was defined as the aggregate biomass of *Loligo* at the end of the season (day 273; September 30th) for north and south sub-areas combined (equations **8** and **9**). Semi-randomized addition of the north and south biomass estimates gave the aggregate likelihood distribution of total escapement biomass shown in Figure 11. The separate north and south escapement biomass distributions had similar forms (Figures 7-right and 9-right), thus total maximum likelihood escapement biomass, and its confidence interval, are nearly equal to their simple addition:

$$
\begin{aligned}
B_{Total\ day\ 273} \quad &\approx \quad B_{N\ day\ 273} \ + \ B_{S\ day\ 273} \\
&= \quad 17{,}250\ t \sim 95\%\ CI\ [13{,}250 - 28{,}500]\ t
\end{aligned} \tag{11}
$$

The risk of the fishery, defined as the proportion of the total escapement biomass distribution below the conservation limit of 10,000 tonnes (Agnew et al., 2002; Barton, 2002), was calculated as effectively zero (Figure 11: the histogram does not extend below 10,000 t).

Immigration

Loligo immigration during the season was inferred as the difference between *Loligo* biomass at the end of the pre-season survey (Winter et al., 2014) and *Loligo* biomass at the end of the commercial season (escapement biomass) plus in-season total catch and natural mortality (equation **A10**). The variability distribution of this difference was calculated by repeated iterations of drawing a random value from the escapement biomass distribution (equation **11**), adding the in-season catch and natural mortality, and subtracting a random draw from the likelihood distribution of the pre-season survey biomass (Winter et al., 2014):

$$
\begin{aligned}
B_{Season\ Immigration} \quad &= \quad B_{Total\ day\ 273} \ + \ C_{Season} \ + \ M_{Season} \ - \ B_{Survey\ end} \\
&= \quad 17{,}250\ [13{,}250 - 28{,}500] \ + \ 19{,}630 \ + \ 12{,}624 \\
&\quad\ - \ 40{,}090\ [30{,}228 - 64{,}677] \\
&= \quad 9{,}414\ t \sim 95\%\ CI\ [0 - 23{,}837]\ t
\end{aligned} \tag{12}
$$

Note that B $_{Season\ Immigration}$ represents, more specifically, the biomass resulting from immigration rather than the biomass that immigrated; it does not taken into account that the squid would have been smaller on the date they entered the fishing zone and subsequently grown. By this estimate, in-season immigration represents 19% of the *Loligo* biomass to have been present in the fishing zone in the 2nd season of 2014: $9,414/(17,250 + 19,630 + 12,624) = 0.190$.

Compared to other seasons, this rate of immigration is on the low end. In-season CPUE peaks were, for the most part, relatively modest, late, and not clearly associated with indicators for new immigration as opposed to aggregation of squid already present (Winter and Arkhipkin, 2012). In a season characterized by the unusual presence of large, older males (see above), it has been conjectured that while these large males may have been inhibited from out-migrating by the high biomass of *Illex* this year (Winter et al., 2014), the cohort of young *Loligo* in 2nd season may in turn have been inhibited from out-migrating by the prolonged presence of the larger, older *Loligo*.
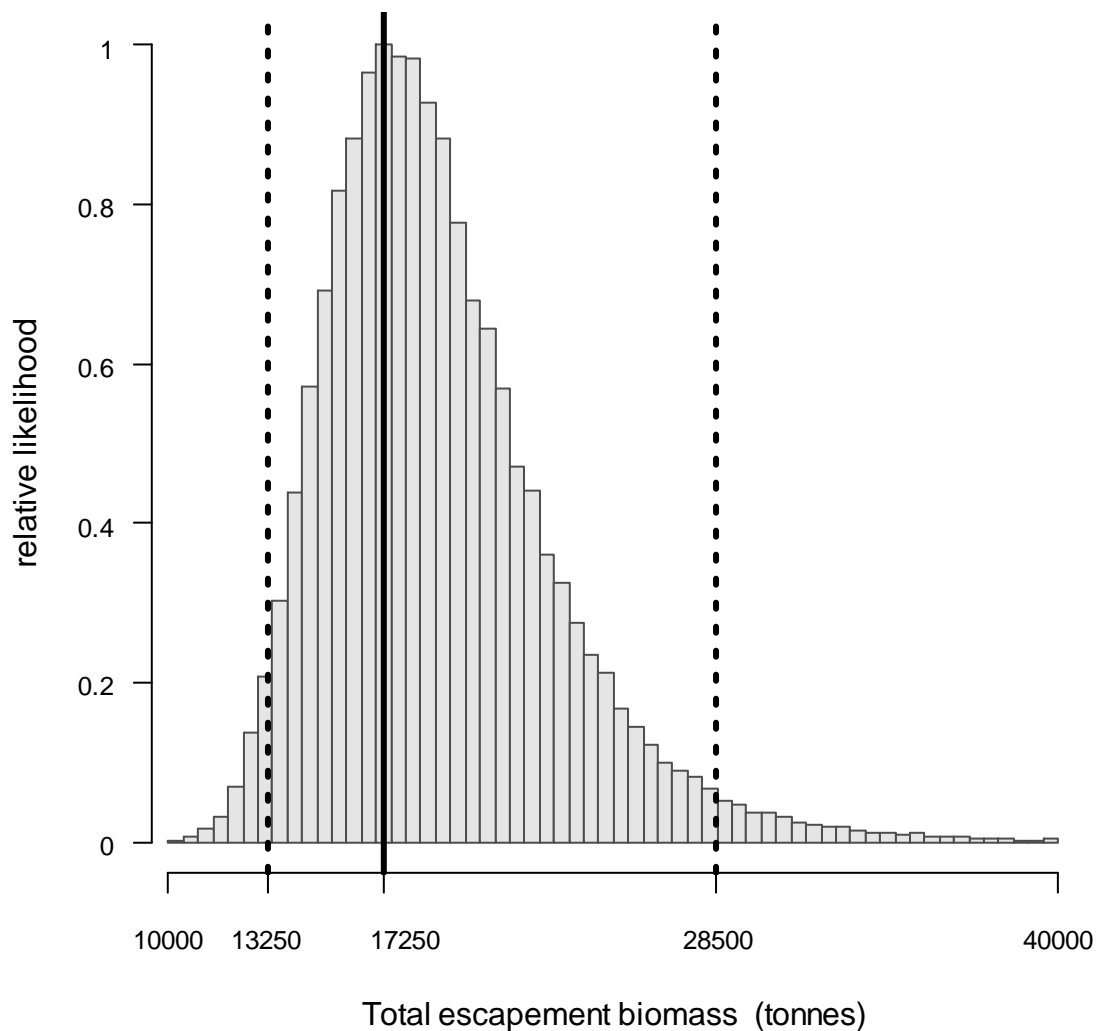

Figure 11. Likelihood distribution with 95% confidence intervals of total *Loligo* escapement biomass at the end of the season (September 30th).

16

Evaluation of season schedule change

The scheduling change of taking the first week off 2nd season (and adding the days to the end of 1st season) was motivated in part by findings that in recent 2nd seasons, *Loligo* catches during that week (July 15th - July 21st) tended to be low. This trend could have two explanations: either any first week of a season is inherently low until vessels have located their target aggregations, or, that calendar week is inherently low as squid have not yet appeared, irrespective of whether vessels are prepared.

To compare trends, 7-day average *Loligo* CPUE were plotted together for all 2nd seasons since 2004. Of the ten 2nd seasons prior to this year, six had CPUE increase from the first week to the second week, including 4 of the 5 most recent prior to this year (Figure 12). The exception of the 5 most recent (2012) still had CPUE of the third week increase above the first week. The current 2014 2nd season, which has eliminated that calendar week, is one of only four in which CPUE decreased from its first week to the second week, and one of only two in which the first week had the season's highest CPUE overall (Figure 12). These data, although not sufficiently numerous for statistical significance, suggest that it is the calendar week of July 15th - July 21st that has low abundance of available *Loligo*, and that this has become prevalent in recent years; perhaps with shifting migratory patterns.
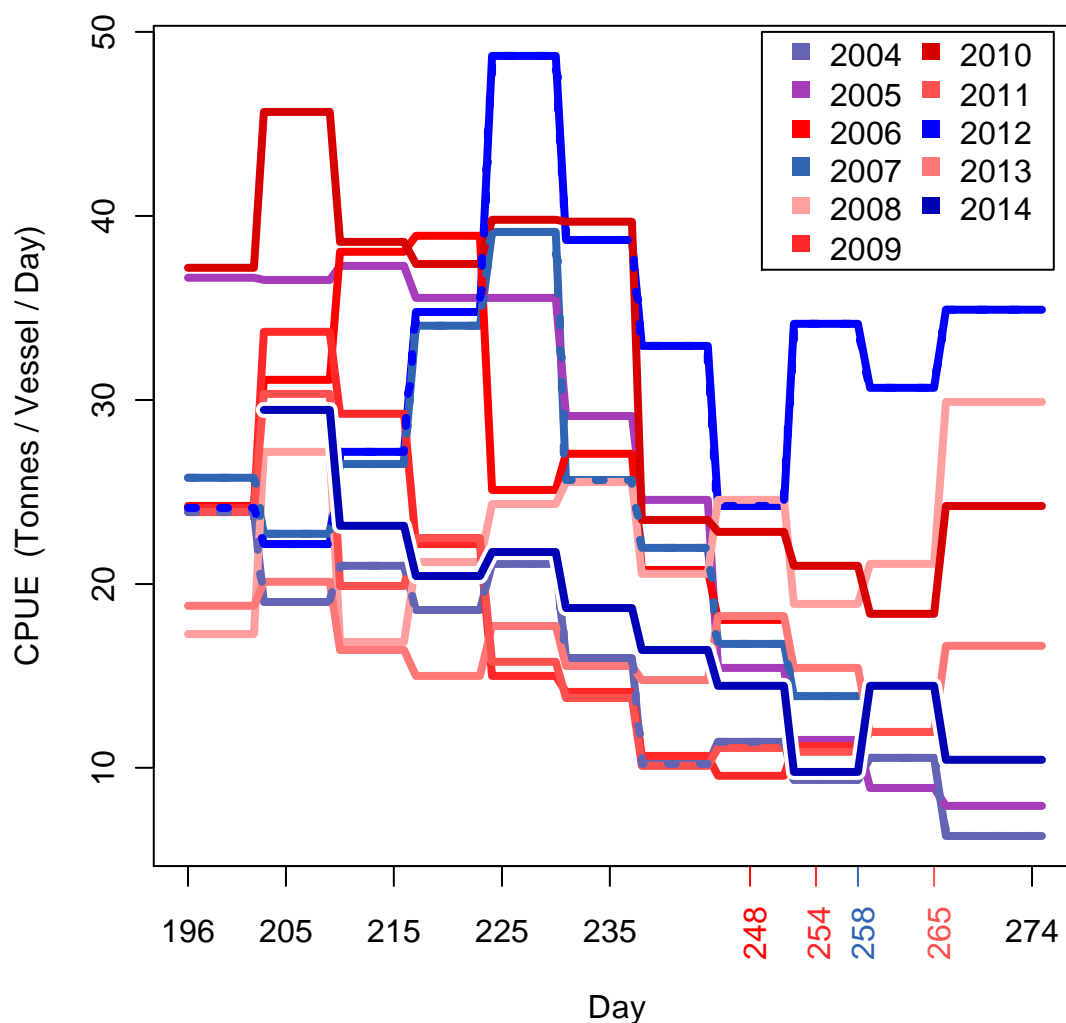
Figure 12 [previous page]. 2nd season time series of *Loligo* CPUE, 2004 to 2014, by 7-day block averages. End dates are indicated for those seasons that were closed before schedule. Red tones are seasons in which CPUE increased from the first to the second week; blue tones are seasons in which CPUE decreased from the first to the second week; purple (2005) – no substantial change from the first to second week. Based on Figure 12 in Winter (2011).

The five previous 2nd seasons (2009-2013) averaged *Loligo* CPUE of 25.8 t vessel-day^{-1} (range 18.8 - 37.1 t vessel-day^{-1}) over the week of July 15th - July 21st. By comparison, the last week of the 2014 1st season (April 15th - April 21st) averaged 36.9 t vessel-day^{-1}, whereby that last week was above average for the season, having had in-season immigrations just before (Winter, 2014). The results suggest that in 2014 the commercial fishery gained substantially from the scheduling change.

Fishing north of the Loligo Box, and bycatch

Over the past few years, vessel operators have requested opportunities to target *Loligo* just north of the Loligo Box (latitude 50.5º S) as catches near the northern boundary of the Loligo Box have suggested high abundances in this area. However, this area is also important habitat for rock cod (*Patagonotothen ramsayi*) (Brickle et al., 2006), and approval has been reserved by concerns that the small-mesh *Loligo* trawls would catch too much rock cod. This season, permission was extended by the FIFD for one vessel with observer coverage to take three exploratory fishing days in grid units XHAL, XJAL, XJAM and XKAN.

Catches of *Loligo* and rock cod of this vessel were compared to the average of vessels fishing in the top three 'rows' of the Loligo Box (between 50.5º S and 51.25º S) on the same days plus one day before and after. These data are shown in Table 2. To avoid identifying the exploratory vessel's catches outright, data are standardized to "1" as the maximum average *Loligo* catch. The vessel north of the Loligo Box averaged lower *Loligo* catch, higher rock cod bycatch, and higher total bycatch than the other vessels inside the north of the Loligo Box (Table 2).

Table 2. Proportional catch (max. 1) of *Loligo* (LOL), rock cod (PAR) and all bycatch of the X-licensed vessel permitted north of the Loligo Box, compared to vessels (N = no. day^{-1}) that fished by regular statute in the northern part of the Loligo Box over the same range of days.

Date	Vessel North of Box				Vessels inside North Box			
	N	LOL	PAR	All By.	N	LOL	PAR	All By.
25/08	0	-	-	-	7	**1.000**	0.115	0.118
26/08	1	0.806	0.204	0.206	10	0.777	0.082	0.084
27/08	1	0.261	0.165	0.260	6	0.734	0.042	0.046
28/08	1	0.633	0.006	0.020	0	-	-	-
29/08	0	-	-	-	4	0.644	0.022	0.023
Avg.		0.567	0.125	0.162		0.806	0.073	0.075

Of the 1099 vessel-days in total (Table 1), 63 reported a primary catch other than *Loligo*: 15 rock cod and 48 blue whiting (*Micromesistius australis*). The four most common commercial bycatches reported overall for the season were rock cod

(1817 t, reported from 973 vessel-days), blue whiting (1677 t, 137 vessel-days), skates (Rajidae) (102 t, 338 vessel-days), and red cod (*Salilota australis*) (88 t, 171 vessel-days). Relative distributions of these bycatches are shown in Figure 13.
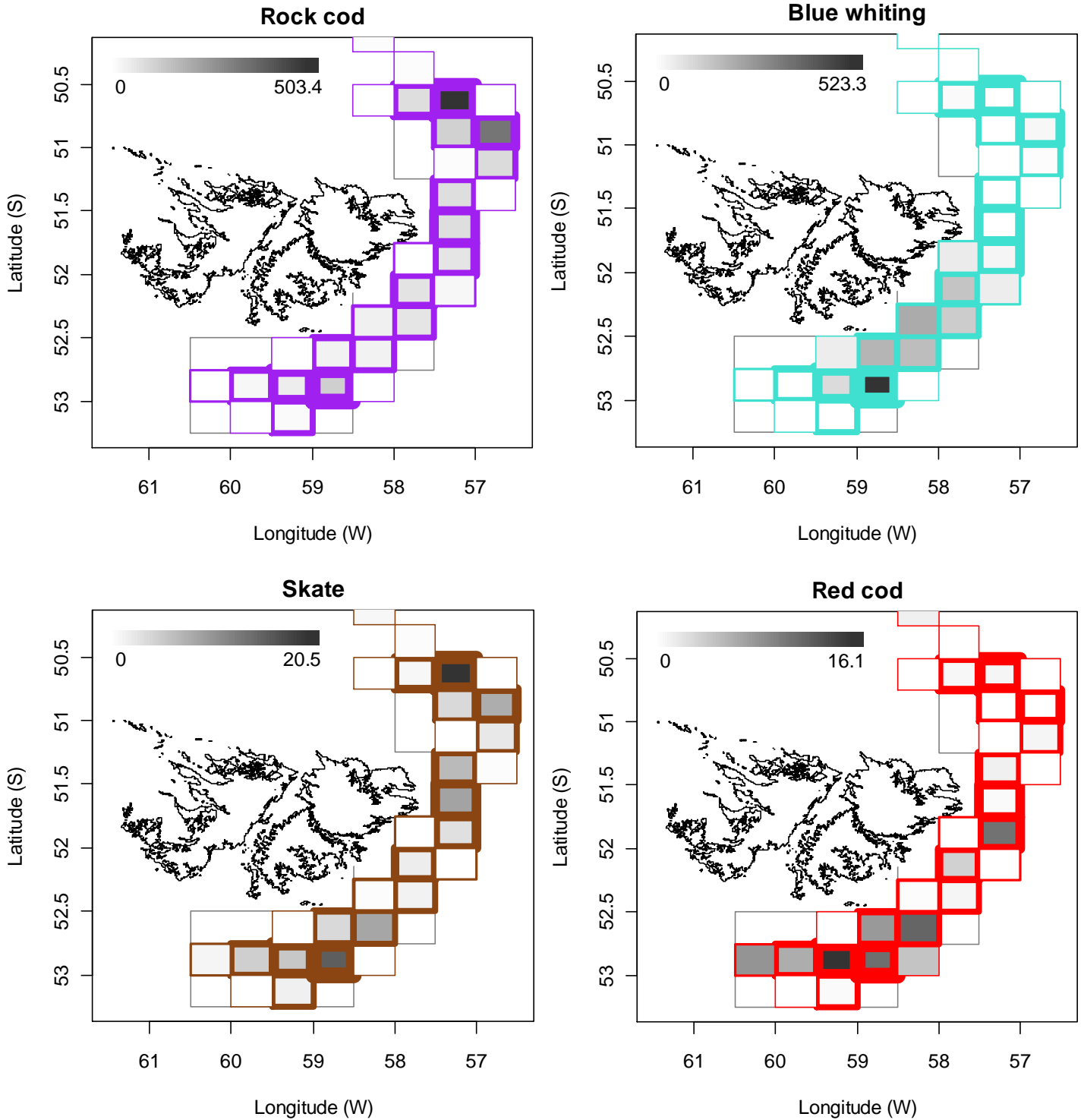

Figure 13. Distributions of the four principal bycatches during 2nd season 2014. Thickness of grid lines is proportional to the number of vessel-days (1 to 184). Gray-scale is proportional to the bycatch biomass; maximum (tonnes) indicated on each plot.

19

References

Agnew, D.J., Baranowski, R., Beddington, J.R., des Clers, S., Nolan, C.P. 1998. Approaches to assessing stocks of *Loligo gahi* around the Falkland Islands. Fisheries Research 35:155-169.

Agnew, D. J., Beddington, J. R., and Hill, S. 2002. The potential use of environmental information to manage squid stocks. Canadian Journal of Fisheries and Aquatic Sciences, 59: 1851–1857.

Arkhipkin, A.I., Middleton, D.A.J. 2002. Sexual segregation in ontogenetic migrations by the squid *Loligo gahi* around the Falkland Islands. Bulletin of Marine Science 71: 109-127.

Arkhipkin, A.I., Middleton, D.A.J., Barton, J. 2008. Management and conservation of a short-lived fishery resource: *Loligo gahi* around the Falkland Islands. American Fisheries Society Symposium 49:1243-1252.

Barton, J. 2002. Fisheries and fisheries management in Falkland Islands Conservation Zones. Aquatic Conservation: Marine and Freshwater Ecosystems, 12: 127–135.

Brickle, P., Laptikhovsky, V., Arkhipkin, A., Portela, J. 2006. Reproductive biology of *Patagonotothen ramsayi* (Pisces: Nototheniidae) around the Falkland Islands. Polar Biology 29: 570-580.

Brooks, S.P., Gelman, A. 1998. General methods for monitoring convergence of iterative simulations. Journal of computational and graphical statistics 7:434-455.

DeLury, D.B. 1947. On the estimation of biological populations. Biometrics 3:145-167.

Gamerman, D., Lopes, H.F. 2006. Markov Chain Monte Carlo. Stochastic simulation for Bayesian inference. 2nd edition. Chapman & Hall/CRC.

Magnusson, A., Punt, A., Hilborn, R. 2013. Measuring uncertainty in fisheries stock assessment: the delta method, bootstrap, and MCMC. Fish and Fisheries 14: 325-342.

Nash, J.C., Varadhan, R. 2011. optimx: A replacement and extension of the optim() function. R package version 2011-2.27. http://CRAN.R-project.org/package=optimx

Patterson, K.R. 1988. Life history of Patagonian squid *Loligo gahi* and growth parameter estimates using least-squares fits to linear and von Bertalanffy models. Marine Ecology Progress Series 47:65-74.

Payá, I. 2010. Fishery Report. *Loligo gahi*, Second Season 2009. Fishery statistics, biological trends, stock assessment and risk analysis. Technical Document, Falkland Islands Fisheries Department. 54 p.

Punt, A.E., Hilborn, R. 1997. Fisheries stock assessment and decision analysis: the Bayesian approach. Reviews in Fish Biology and Fisheries 7:35-63.

Roa-Ureta, R. 2012. Modelling in-season pulses of recruitment and hyperstability-hyperdepletion in the *Loligo gahi* fishery around the Falkland Islands with generalized depletion models. ICES Journal of Marine Science, 69: 1403–1415.

Roa-Ureta, R., Arkhipkin, A.I. 2007. Short-term stock assessment of *Loligo gahi* at the Falkland Islands: sequential use of stochastic biomass projection and stock depletion models. ICES Journal of Marine Science 64:3-17.

Rosenberg, A.A., Kirkwood, G.P., Crombie, J.A., Beddington, J.R. 1990. The assessment of stocks of annual squid species. Fisheries Research 8:335-350.

Winter, A., Arkhipkin, A. 2012. Predicting recruitment pulses of Patagonian squid in the Falkland Islands fishery. World Fisheries Congress, Edinburgh, Scotland.

Winter, A. 2011. *Loligo gahi* stock assessment, second season 2011. Technical Document, Falkland Islands Fisheries Department. 28 p.

Winter, A. 2014. *Loligo* stock assessment, first season 2014. Technical Document, Falkland Islands Fisheries Department. 30 p.

Winter, A., Jones, J., Herrera, D. 2014. *Loligo* stock assessment survey, 2nd season 2014. Technical Document, Falkland Islands Fisheries Department. 22 p.

Zhang, H.-M., Bates, J.J., Reynolds, R.W. 2006. Assessment of composite global sampling: Sea surface wind speed. Geophysical Research Letters, 33: L17714.

Appendix
Prior estimates and CV

The pre-season survey (Winter et al., 2014) had estimated *Loligo* biomasses of 17,877 t (standard deviation: ± 4,699 t) north of 52º S and 22,213 t (standard deviation: ± 5,364 t) south of 52º S. From modelled survey catchability, Payá (2010) had estimated average net escapement of up to 22%, which was added to the standard deviation:

$$17,877 \pm \left(\frac{4,699}{17,877} + .22 \right) \; = \; 17,877 \pm 48.3\% \; = \; 17,877 \pm \; 8,631 \; \text{t.} \qquad \textbf{(A1-N)}$$

$$22,213 \pm \left(\frac{5,364}{22,213} + .22 \right) \; = \; 22,213 \pm 46.1\% \; = \; 22,213 \pm 10,250 \; \text{t.} \qquad \textbf{(A1-S)}$$

The 22% was added as a linear increase in the variability, but was not used to reduce the total estimate, because *Loligo* that escape one trawl are likely to be part of the biomass concentration that is available to the next trawl. This estimate in biomass was converted to an estimate in numbers using the size-frequency distributions sampled during the pre-season survey (Winter et al., 2014).

 Loligo were sampled at 57 pre-season survey stations, giving average mantle lengths (both sexes; weighted for *Loligo* density distribution) of 14.34 cm north and 13.09 cm south, corresponding to respectively 0.058 and 0.047 kg average individual weight. Variability distributions of average individual weight were estimated by randomly re-sampling the length-frequency data 10,000×, giving coefficients of variation 1.52% north and 1.16% south. Average coefficients of variation of the length-weight relationship (equation **7**) were 6.96% north and 6.31% south. Combining all sources of variation with the pre-season survey biomass estimates and average individual weights gave estimated *Loligo* numbers at season start (July 22nd; day 203) of:

$$_{\text{prior}} N_{\text{N day 203}} \quad = \quad \frac{17,877 \times 1000}{0.058} \pm \sqrt{48.3\%^{2} + 1.52\%^{2} + 6.96\%^{2}}$$

$$= \; 0.304 \times 10^{9} \pm 48.8\% \; = \; 0.304 \times 10^{9} \pm 0.149 \times 10^{9} \qquad \textbf{(A2-N)}$$

$$_{\text{prior}} N_{\text{S day 203}} \quad = \quad \frac{22,213 \times 1000}{0.047} \pm \sqrt{46.1\%^{2} + 1.16\%^{2} + 6.31\%^{2}} \qquad \text{[lolassess\_2\_priors.R]}$$

$$= \; 0.466 \times 10^{9} \pm 46.6\% \; = \; 0.466 \times 10^{9} \pm 0.217 \times 10^{9} \qquad \textbf{(A2-S)}$$

The catchability coefficient (q) prior for the north sub-area was taken on day 205, when 10 vessels were fishing north and the first depletion period north started:

$$_{\text{prior}} q_{\text{N}} \qquad = \; C(N)_{\text{N day 205}} / (_{\text{prior}} N_{\text{N day 205}} \; \times \; E_{\text{N day 205}})$$

$$= \; (C(B)_{\text{N day 205}} / Wt_{\text{N day 205}}) / (_{\text{prior}} N_{\text{N day 205}} \; \times \; E_{\text{N day 205}})$$

$$= \; (314.1 \; \text{t} / 0.082 \; \text{kg}) / (0.296 \times 10^{9} \; \times \; 9.75 \; \text{vessel-days})$$

$$= \; 1.346 \times 10^{-3} \; \text{vessels}^{-1} \qquad \textbf{(A3-N)}$$

The catchability coefficient prior for the south sub-area was taken on day 203, the first day of the season, when 14 vessels were fishing south. This was preferred over the start of the first depletion period south (day 209), which was 6 days removed from the end of the survey, making the connection more tenuous, and only 4 vessels were fishing south that day.

$$
\begin{aligned}
_{prior}q_S \quad &= C(N)_{S\,day\,203} / (_{prior}N_{S\,day\,203} \times E_{S\,day\,203}) \\
&= (C(B)_{S\,day\,203} / Wt_{S\,day\,203}) / (_{prior}N_{S\,day\,203} \times E_{S\,day\,203}) \\
&= (491.8\,t / 0.054\,kg) / (0.466 \times 10^9 \times 14\,vessel\text{-}days) \\
&= 1.392 \times 10^{-3}\ vessels^{-1} \quad\quad\quad\quad\quad \textbf{(A3-S)}
\end{aligned}
$$

CVs of the priors were calculated as the sums of variability in $_{prior}N$ (equations **A2**) plus variability in the catches of vessels on the q days (day 205 N and day 203 S):

$$
CV_{prior\,N} = \sqrt{48.8\%^2 + \left(\frac{SD\left(C(B)_{N\,vessels\,day\,205}\right)}{mean\left(C(B)_{N\,vessels\,day\,205}\right)} \right)^2}
$$

$$
= \sqrt{48.8\%^2 + 25.6\%^2} = 55.1\% \quad\quad\quad\quad \textbf{(A4-N)}
$$

$$
CV_{prior\,S} = \sqrt{46.6\%^2 + \left(\frac{SD\left(C(B)_{S\,vessels\,day\,203}\right)}{mean\left(C(B)_{S\,vessels\,day\,203}\right)} \right)^2}
$$

$$
= \sqrt{46.6\%^2 + 21.7\%^2} = 60.0\% \quad\quad\quad\quad \textbf{(A4-S)}
$$

Depletion model estimates and CV

For the north sub-area, the equivalent of equation **2** with three N_{day} was optimized on the difference between predicted catches and actual catches (equation **3**), resulting in:

$$
_{depletion}N1_{N\,day\,205} = 0.276 \times 10^9; \quad\quad _{depletion}N2_{N\,day\,228} = 0.128 \times 10^9
$$

$$
_{depletion}N3_{N\,day\,261} = 0.089 \times 10^9
$$

$$
_{depletion}q_N = 1.593 \times 10^{-3}\ vessels^{-1} \quad\quad\quad\quad \textbf{(A5-N)}
$$

These parameters produced the fit between predicted and actual catches shown in Figure A1-N. The root-mean-square deviation of predicted vs. actual catches was calculated and divided by the mean actual catch to give:

$$
CV_{rmsd\,N} = \frac{\sqrt{\sum\limits_i \left(_{predicted}C(N)_{N\,day\,i} - _{actual}C(N)_{N\,day\,i}\right)^2}}{mean\left(_{actual}C(N)_{N\,day\,i}\right)}
$$

$$
= 5.194 \times 10^5 / 2.292 \times 10^6 = 22.7\% \quad\quad\quad\quad \textbf{(A6-N)}
$$

$CV_{rmsd\ N}$ was added to the variability in depletion optimization inferred from variability in the daily average individual *Loligo* weights. In previous assessments, variability in daily average individual *Loligo* weights had been included as a randomized multiplicative factor of the MCMC distribution of *Loligo* numbers, to estimate biomass variability. However, *Loligo* numbers are derived in part from *Loligo* weights rather than being statistically independent, and therefore a truer measure of biomass variability may be obtained by estimating the effect of weight variation in the original depletion optimization.
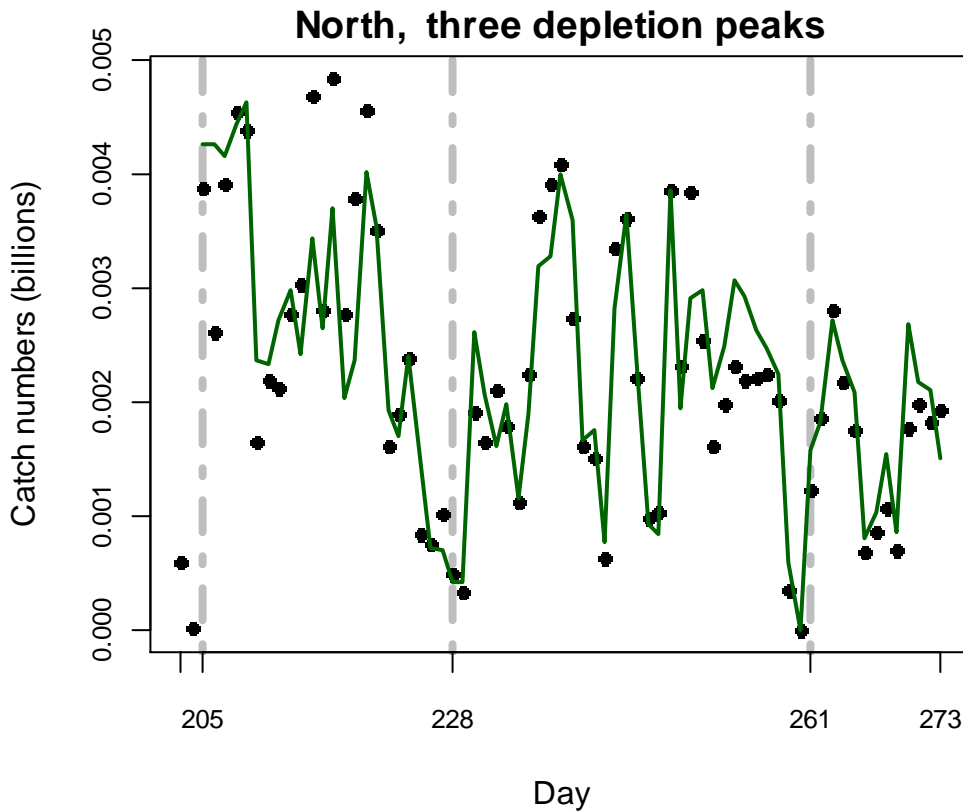

Figure A1-N. Daily catch numbers estimated from actual catch (black points) and predicted from the depletion model (green line) in the north sub-area.

Figure A2-N shows the season time series of individual *Loligo* weights in the north sub-area. A generalized additive model (GAM) was calculated for the daily average individual *Loligo* weight trend. Random permutation of residual differences between GAM-predicted vs. recorded daily average individual weights was used to create re-samples of estimated catch numbers per day ($C(N)_{day} = C(B)_{day} /\ _{avg}Wt_{day}$), which were then entered in the depletion optimization. This process was iterated 1000×. The optimized q value was retained from each iteration and the variability of the optimization with respect to average individual weight calculated as:

$$CV_{optim\ Wt\ N} \quad = \frac{sd\left(q_{perm\ N}\right)}{mean\left(q_{perm\ N}\right)} \quad =\ 11.2\% \qquad \textbf{(A7-N)}$$

CVs of the depletion were then calculated as the sum:

$$\text{CV}_{\text{depletion N}} \quad = \sqrt{\text{CV}_{\text{rmsd N}}^2 + \text{CV}_{\text{optim Wt N}}^2} \quad = \sqrt{22.7\%^2 + 11.2\%^2}$$
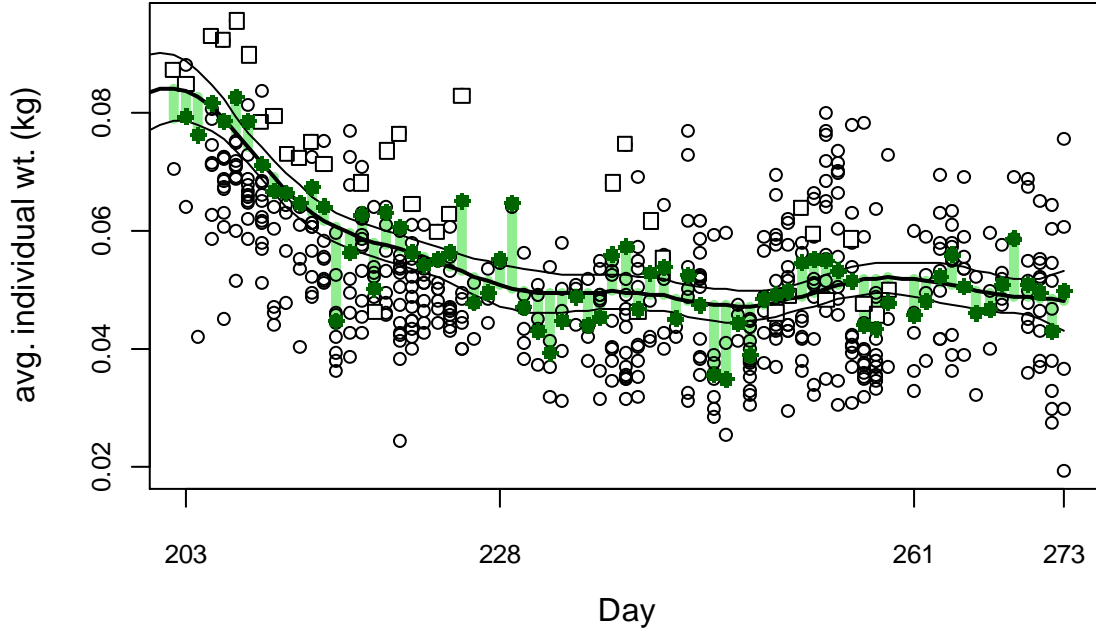
$$= \quad 25.3\% \qquad \textbf{(A8-N)}$$

Figure A2-N. North sub-area daily average individual *Loligo* weights from commercial size categories per vessel (circles), observer measurements (squares), combined daily averages (green circles), GAM of the daily trend ± 95% conf. int. (black lines), and residual differences between the combined daily averages and GAM (light green bars).

For the south sub-area, the equivalent of equation **2** with three N $_{\text{day}}$ was optimized on the difference between predicted catches and actual catches (equation **3**), resulting in parameters values:

$$_{\text{depletion}} N1_{\text{S day 209}} \quad = 0.448 \times 10^9; \qquad _{\text{depletion}} N2_{\text{S day 226}} \quad = 0.095 \times 10^9$$

$$_{\text{depletion}} N3_{\text{S day 258}} \quad = 0.065 \times 10^9$$

$$_{\text{depletion}} q_{\text{S}} \quad = 1.405 \times 10^{-3} \text{ vessels}^{-1} \qquad \textbf{(A5-S)}$$

These parameters produced the fit between predicted and actual catches shown in Figure A1-S. The root-mean-square deviation of predicted vs. actual catches was calculated, and its CV assigned to the depletion model q parameter:

$$\text{CV}_{\text{rmsd S}} \quad = \frac{\sqrt{\sum_i \left(_{\text{predicted}} C(N)_{\text{S day i}} -_{\text{actual}} C(N)_{\text{S day i}}\right)^2}}{\text{mean}\left(_{\text{actual}} C(N)_{\text{S day i}}\right)}$$

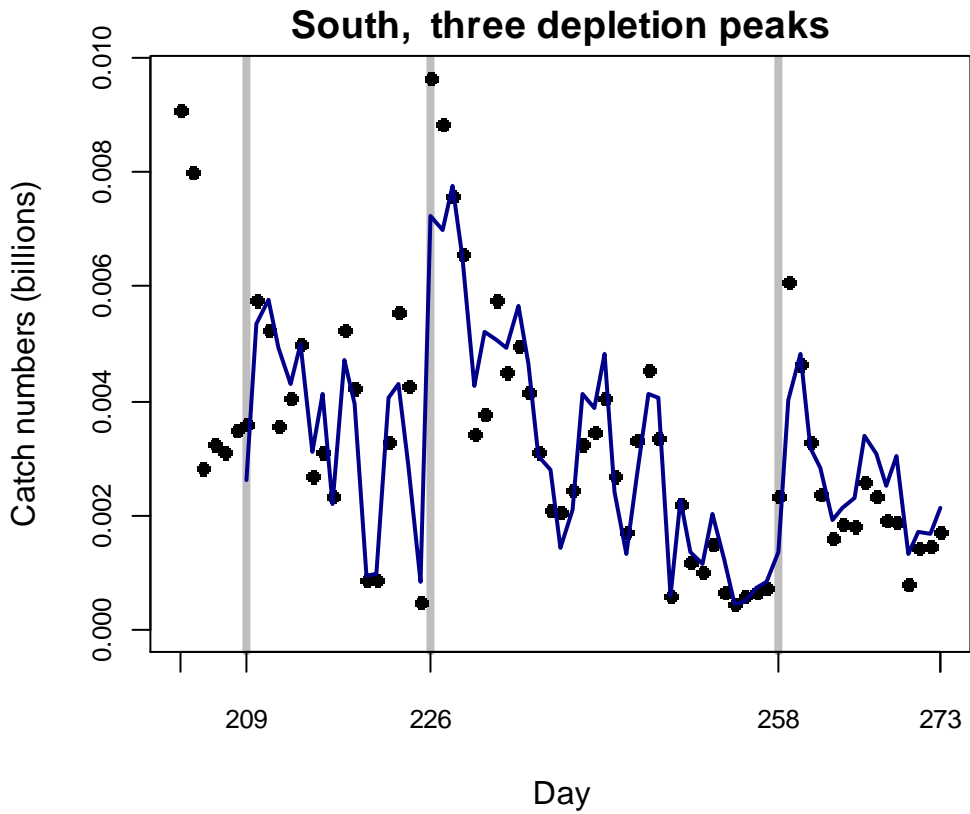$$= 7.477 \times 10^5 / 3.137 \times 10^6 = 23.8\% \qquad \textbf{(A6-S)}$$

Figure A1-S. Daily catch numbers estimated from actual catch (black points) and predicted from the depletion model (blue line) in the south sub-area.
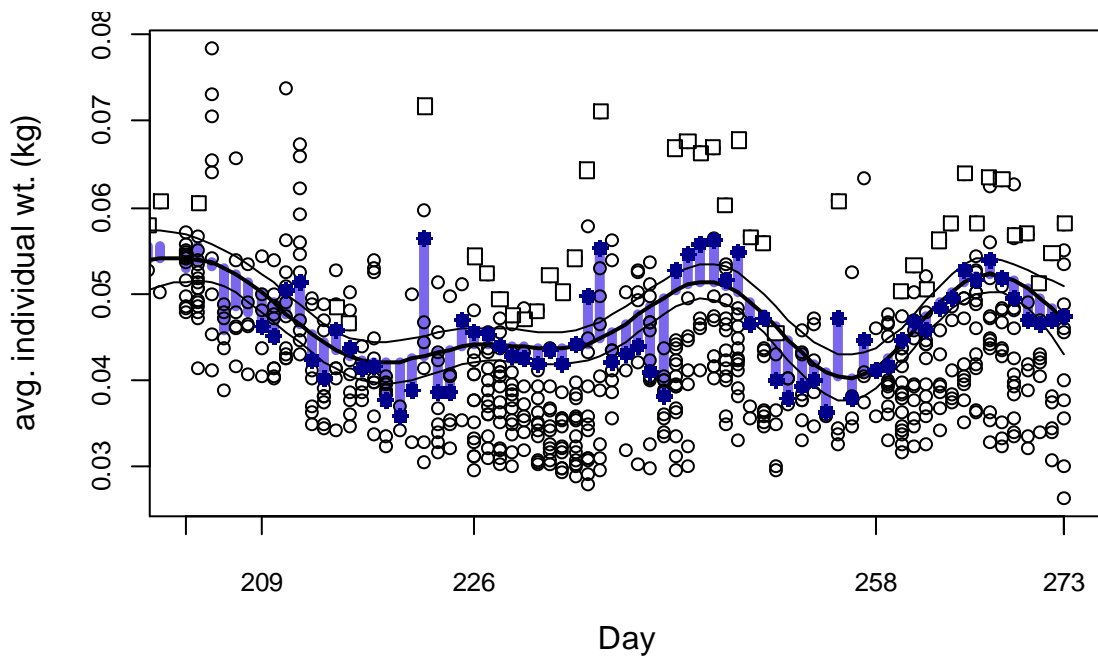

Figure A2-S. South sub-area daily average individual *Loligo* weights from commercial size categories per vessel (circles), observer measurements (squares), combined daily averages (blue circles), GAM of the daily trend ± 95% conf. int. (black lines), and residual differences between the combined daily averages and GAM (light blue bars).

$\text{CV}_{\text{rmsd S}}$ was added to the variability in depletion optimization inferred from variability in the daily average individual *Loligo* weights (Figure A2-S):

$$\text{CV}_{\text{optim Wt S}} = \frac{\text{sd}\left(q_{\text{perm S}}\right)}{\text{mean}\left(q_{\text{perm S}}\right)} = 10.0\% \qquad \textbf{(A7-S)}$$

CVs of the depletion were then calculated as the sum:

$$\text{CV}_{\text{depletion S}} = \sqrt{\text{CV}_{\text{rmsd S}}{}^2 + \text{CV}_{\text{optim Wt S}}{}^2} = \sqrt{23.8\%^2 + 10.0\%^2}$$
$$= 25.8\% \qquad \textbf{(A8-S)}$$

Semi-randomized addition of north and south escapement biomass likelihood distributions

North and south depletion model biomass time series estimates were quite similar (Figures 8 and 10), counter to an assumption that they are independent. The correlation coefficient of north and south biomasses was:

$$r\left(B_{\text{N day 203-273}}, B_{\text{S day 203-273}}\right) = +0.8402 \qquad \textbf{(A9)}$$

To incorporate this correlation in the addition of the north and south escapement biomasses, the highest common number of iterations was taken from the respective north and south likelihood distributions (because of the variable MCMC thinning algorithm (see Methods), they were not necessarily identical). These were separately ordered by magnitude of the iterations. Then, each ordered iteration of the south escapement biomass[1] was randomly flagged for either permutation or not, in proportion to the correlation; i.e., each iteration had a 1 - 0.8402 = 0.1598 probability of being flagged for permutation. Then, the subset of all flagged iterations was randomly permuted. Then, the ordered set of north escapement biomass likelihood iterations, and the ordered, flagged, and partially permuted set of south escapement biomass likelihood iterations, were added together. The process was replicated 7× for greater statistical power.

Limit expectations of this algorithm are that if correlation had been zero, then 1 – 0 = all of the iterations would have been permuted, and the addition of the north and south sets of likelihood iterations would have been fully randomized. If correlation had been 100%, then 1 – 1 = none of the iterations would have been permuted, and the north and south sets of likelihood iterations would have been added together fully ordered; i.e. the smallest value of the north set plus the smallest value of the south set, the 2nd-smallest value of the north set plus the 2nd-smallest value of the south set, etc. If the biomass time series correlation $r\left(B_{\text{N day 203-273}}, B_{\text{S day 203-273}}\right)$ had been negative, then one of the two sets of north or south likelihood iterations would have been reverse-ordered so that their addition would have been back-to-front, notwithstanding the degree of permutation.

---

[1] Whereby it is arbitrary whether this was done with the south or north likelihood iterations. What matters is the degree of randomization of one relative to the other.

In-season mortality estimation.
For consistency, model-estimate *Loligo* numbers on each day of the season were back-calculated from the Bayesian posterior maximum likelihood of daily biomass estimates (as presented in Figures 8 and 10), divided by the daily GAM estimate of average individual weight to give maximum likelihood numbers. To calculate daily natural mortality, these numbers were then multiplied by the natural mortality rate $\times$ ½ (implying that the mortality was gathered at mid-day, so that the squid had a 50% chance of having been available to catch before they died):

$$N_{N\ day\ 203\text{-}273} = B_{N\ day\ 203\text{-}273} / Wt_{N\ day\ 203\text{-}273}$$

$$M(N)_{N\ day\ 203\text{-}273} = N_{N\ day\ 203\text{-}273} \times (1 - e^{-M/2})$$

$$M(B)_{N\ day\ 203\text{-}273} = M(N)_{N\ day\ 203\text{-}273} \times Wt_{N\ day\ 203\text{-}273}$$

$$N_{S\ day\ 203\text{-}273} = B_{S\ day\ 203\text{-}273} / Wt_{S\ day\ 203\text{-}273}$$

$$M(N)_{S\ day\ 203\text{-}273} = N_{S\ day\ 203\text{-}273} \times (1 - e^{-M/2})$$

$$M(B)_{S\ day\ 203\text{-}273} = M(N)_{S\ day\ 203\text{-}273} \times Wt_{S\ day\ 203\text{-}273}$$

Because the depletion models were not started right away on the first day of the season (day 203), M(B) on the initial days before model start were approximated as the same as the first day on which the model was started. Then:

$$M_{Season\ N} = \Sigma\ M(B)_{N\ day\ 203\text{-}273} = 5{,}978\ t$$

$$M_{Season\ S} = \Sigma\ M(B)_{S\ day\ 203\text{-}273} = 6{,}646\ t$$

$$M_{Season} = M_{Season\ N} + M_{Season\ S} = 12{,}624\ t \qquad \textbf{(A10)}$$

Note that calculation of the variability distribution for equation **12** is simplified insofar as the values of M, N, and Wt are all treated as fixed parameters in the randomization, and their own error distributions as model estimates are not addressed.